Available online at www.sciencedirect.com
ScienceDirect
Journal of the European Ceramic Society 30 (2010) 1317–1325
www.elsevier.com/locate/jeurceramsoc

Effect of TiO_2 doping on the characteristics of macroporous Al_2O_3/TiO_2 membrane supports

Hong Qi [a,*], Yiqun Fan [a], Weihong Xing [a], Louis Winnubst [b]

[a] State Key Laboratory of Materials-Oriented Chemical Engineering, Membrane Science and Technology Research Center, Nanjing University of Technology, No. 5 New Model Road, Nanjing 210009, China

[b] Inorganic Membranes, Membrane Technology Group, MESA+ Institute for Nanotechnology, University of Twente, P.O. Box 217, 7500 AE Enschede, The Netherlands

Received 2 August 2009; received in revised form 17 November 2009; accepted 17 December 2009
Available online 12 January 2010

Abstract

A cost-effective tubular macroporous ceramic support consisting of alumina and titania was prepared by extrusion and subsequent heat treatment. An Al_2O_3/TiO_2 composite support with high porosity (41.4%), an average pore size of 6.8 μm and sufficient mechanical strength (32.7 MPa) was obtained after sintering at 1400 °C. The formation mechanism of this support as investigated with X-ray micromapping, SEM and XRD indicated that the appearance of Al_2TiO_5 plays a key role in the fabrication of high performance composite membrane supports at relatively low temperature. The amount of Al_2TiO_5 present in the composite has a strong impact on the properties of supports, especially with regard to the mechanical strength. A composite of 85 wt.% Al_2O_3/15 wt.% TiO_2 sintered at 1400 °C for 2 h exhibited both high permeability (pure water flux of 45 $m^3\ m^{-2}\ h^{-1}\ bar^{-1}$), together with an excellent corrosive resistance towards hot NaOH and HNO_3 solutions.

Keywords: Ceramic membranes; Macroporous support; Al_2O_3; TiO_2; Al_2TiO_5

1. Introduction

Since their introduction to commercial applications in the early 1980s, owing to their thermal, mechanical and chemical stability, ceramic membranes are making rapid progress in many areas such as food and beverage processing, biotechnology applications and water treatment.[1,2] However, the disadvantages such as high cost and low surface area to module volume ratio[3] greatly restrict its broad application. Ceramic membranes generally consist of several thin separation layers with thicknesses between a few tens of nanometers up to a few microns superimposed on a macroporous support. The support provides mechanical strength to the top membrane layer and must simultaneously have a high permeation and a high corrosion resistance to the filtrate flow.[4] The high costs of ceramic membranes are partly attributed to the macroporous ceramic support, which is prepared via extrusion with subsequent drying and sintering processes. To impart the membrane support with sufficient mechanical strength as well as high permeability, most of the commercial macroporous ceramic supports (e.g. Membralox®, Cefilt®) were made from alumina powders with particle size in the range of 20–40 μm. Because of the extremely low sintering activity of these coarse-grained alumina, no sufficient strength could be obtained unless the sintering temperature reaches 1700 °C, or even higher.[5]

In order to fabricate these types of ceramic membrane supports at low sintering temperatures, several methods were proposed in the last 2 decades. A general method was to fabricate with starting powder of cordierite,[6] mullite[7] or a composite of alumina/clay,[8,9] whose sintering temperatures were all much lower than that of pure alumina.[10,11] To modify the powders with improved sintering activity so as to reduce the sintering temperature of the membrane support was also put forward as an alternative approach.[12,13] Nevertheless, in order to design membrane supports, one must keep in mind the integrative properties, i.e. sufficient permeability as well as mechanical and chemical stability.[14] Most of the studies with respect to membrane support are focused on either permeability or mechanical property, while one of the most important parameters, the corrosion resistance of the support was seldom studied. Therefore, inventive solutions in

* Corresponding author. Tel.: +86 25 83172279; fax: +86 25 83172292.
E-mail address: hqinjut@yahoo.com.cn (H. Qi).

0955-2219/$ – see front matter © 2009 Elsevier Ltd. All rights reserved.
doi:10.1016/j.jeurceramsoc.2009.12.011

Table 1
Chemical analysis of alumina and titania powders.

Oxide	Alumina (wt.)	Titania (wt.)
SiO_2	350 ppm	0.3%
Fe_2O_3	300 ppm	200 ppm
MnO	<100 ppm	<100 ppm
MgO	<100 ppm	200 ppm
CaO	100 ppm	200 ppm
Na_2O	0.19%	0.25%
K_2O	250 ppm	200 ppm

designing commercial low-cost macroporous ceramic supports with high performance (integrated properties of permeability, mechanical and chemical stability) are still in progress.[7,9]

α-Al_2O_3 and TiO_2 are normally used as membrane materials because of their excellent chemical stability towards extreme pH conditions. More important, it was reported[15] that alumina and titania could form aluminum titanate through solid-state reactions above 1280 °C. The appearance of aluminum titanate in the Al_2O_3/TiO_2 system increases the concentration of vacancies and accordingly the velocity of mass transfer.[16,17] The required properties for membrane supports such as sufficient mechanical strength as well as high permeability could be simultaneously obtained at a remarkably low temperature. Although the fabrication of porous alumina/titania membrane supports has been reported,[18–20] few studies are available with respect to the formation mechanism of the Al_2TiO_5 phase and the effect of sintering temperature on support properties.

In this paper we report the microstructural characteristics and mechanical properties of tubular macroporous ceramic membrane supports consisting of alumina and titania made by extrusion while sintered at a comparative low temperature.

2. Experimental

2.1. Characterization of the starting powders

α-Al_2O_3 (purity > 99.5%, Zhengzhou, China) and TiO_2 (purity > 99%, Nanjing, China) powders were used as received. Table 1 shows the chemical analysis (determined by sequential X-ray fluorescence spectrometer, XRF, VF-320, Shimadzu, Japan) of these starting powders. Fig. 1 depicts the alumina and titania particle size distributions as measured by dynamic light scattering (DLS) using Mastersizer 2000 apparatus (Malvern Instrument Co., Ltd., UK). The average size of α-Al_2O_3 and TiO_2 was ~30 μm and ~0.5 μm, respectively.

2.2. Preparation of the tubular macroporous supports

The above-mentioned Al_2O_3 and TiO_2 powders were first mixed for 1 h in a ball mill (QMM/B, Xianyang Jinhong Mechanical Co. Ltd., China) with Al_2O_3 ball and ethanol (the weight ratio for the inorganic powders:Al_2O_3 ball:ethanol was 1:1.5:0.8). Subsequently various organic additives including binders (carboxymethyl cellulose, 2 wt.% with respect to the mixture of Al_2O_3 and TiO_2; all wt.% are relative to the amount

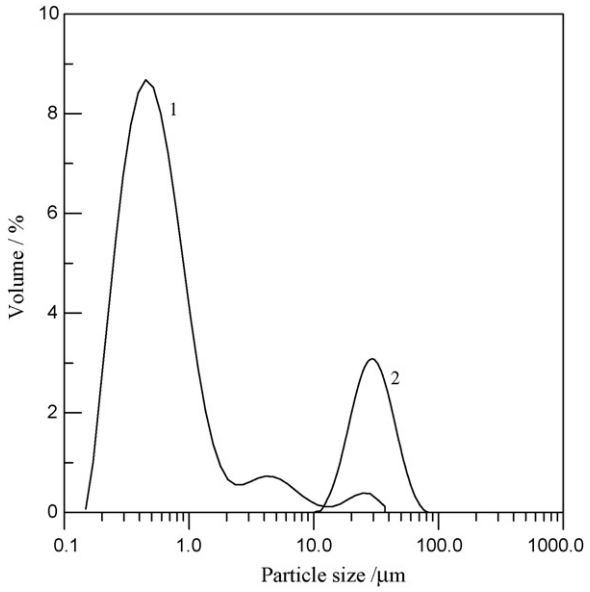

Fig. 1. Particle size distributions of titania (1) and alumina (2) powders.

of inorganic powder), plasticizer (polyvinylalcohol, 10 wt.%), lubricant (glycerine, 7.5 wt.%) and solvent (water, 4.5 wt.%) were slowly added to the powder mixture. The powders plus additives were subsequently purged under vacuum (−0.1 MPa) for 1 h to obtain a homogeneous paste suitable for extrusion. Extrusion was performed at a pressure of 4 MPa using a home-made extruder equipped with a de-gassing device. The extruded tubular green supports (O.D.: 12 mm; I.D.: 8 mm) were dried and sintered in an electrical furnace (SX_2-14-17, Wuxi Universal Electrical Machine Works Co., Ltd., China) under air. Four kinds of tubular supports with different compositions are hereafter referred as A100/0 (Al_2O_3/TiO_2 = 100/0, weight ratio), A95/5 (Al_2O_3/TiO_2 = 95/5), A85/15 (Al_2O_3/TiO_2 = 85/15) and A70/30 (Al_2O_3/TiO_2 = 70/30). At the end of each sintering cycle, some supports were taken out from the furnace and air-quenched, while others were cooled down at a rate of 3 °C/min in the furnace to the ambient temperature. The sintered supports with different cooling mode were hereafter designated as A100/0(AQ)–A70/30(AQ) for air-quenched mode and A100/0–A70/30 for cooling down in the furnace to the ambient temperature at a rate of 3 °C/min.

2.3. Characterization of the macroporous supports

The density of sintered supports was determined using Archimedes method with water as immersion medium. Pore size distribution of supports and membranes was measured by a gas bubble pressure method.[21] Permeability of supports as well as membranes was characterized by pure water flux using cross-flow filtration equipment under various transmembrane pressures (0.05–0.3 MPa) at 25 °C. A plot of permeability ($m^3\ m^{-2}\ h^{-1}$) versus transmembrane pressure (bar) is then obtained and the pure water flux ($m^3\ m^{-2}\ h^{-1}\ bar^{-1}$) of the support/membrane can be calculated from these results. Scanning electron microscope (SEM, JSM-6300, JEOL) was employed

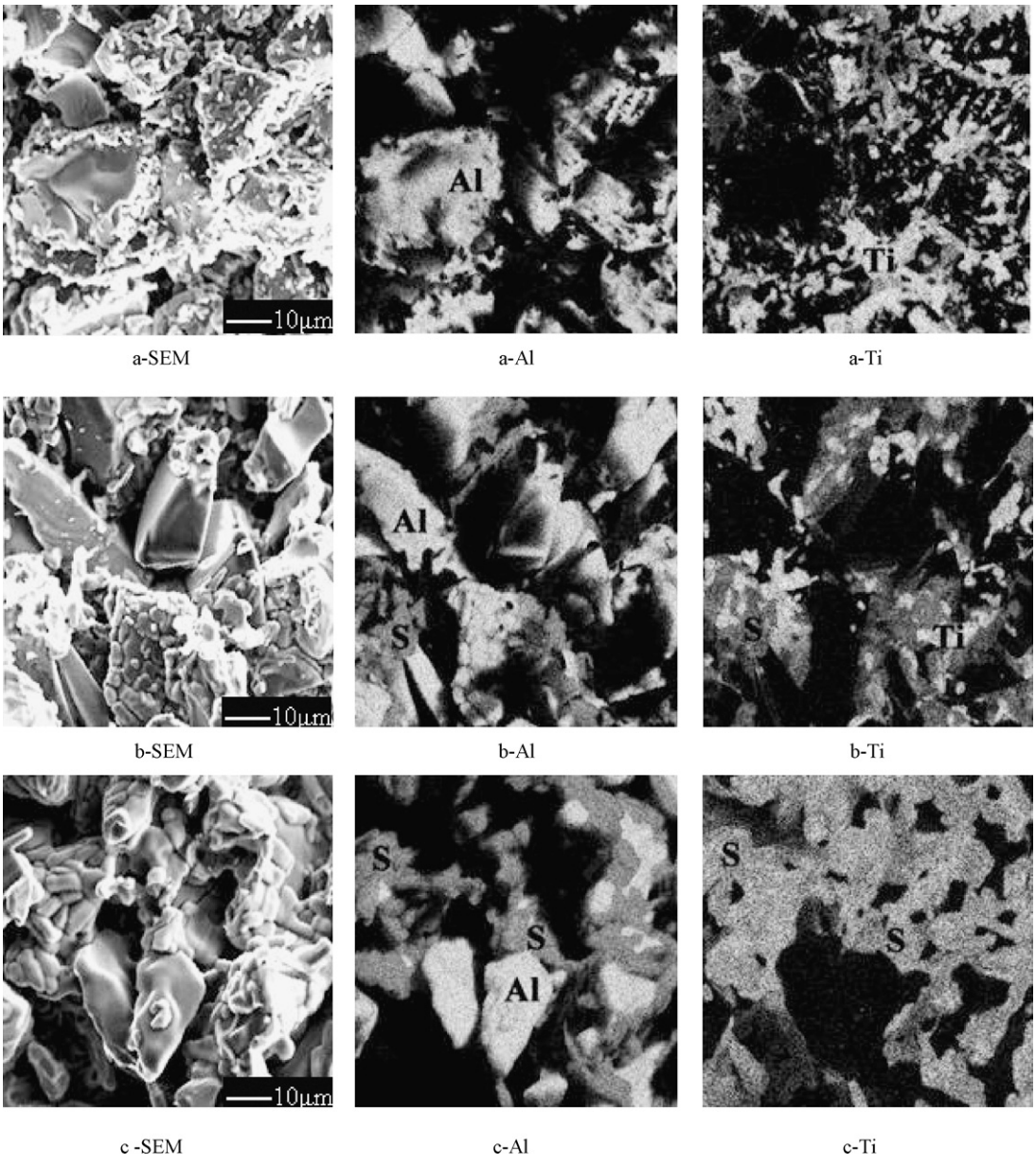

Fig. 2. SEM photos and corresponding micromaps of support A85/15(AQ) sintered at 1300 °C (a-SEM, a-Al, a-Ti), 1400 °C (b-SEM, b-Al, b-Ti) and 1500 °C (c-SEM, c-Al, c-Ti). Al, Al_2O_3; Ti, TiO_2; S, Al_2TiO_5. The analysis area is 80 μm × 80 μm.

to observe surfaces of fractured samples as well as the inner surface section of supports and membranes. X-ray micromapping (attached to the SEM, JSM-6300, JEOL) on selected areas (80 μm × 80 μm) was used to evaluate the Al and Ti elemental distribution of the sintered supports. For each support 3 areas of 80 μm × 80 μm were analyzed by EDX. The phase composition of sintered supports was probed by X-ray diffraction (XRD, DMAX-RB diffractometer, Rigaku, Japan) with Cu Kα radiation. The mechanical strength of tubular supports was determined based on the three point bending method.[2] A support with 120 mm in length and 12 mm × 8 mm (O.D. × I.D.) in cross section was placed on two stainless-steel jigs 100 mm apart. Samples were bent and fractured by an upper stainless-steel jig, at a constant loading rate of 550 N/min. The three point bending strength of supports was calculated by the following equation[22]:

$$R_f = \frac{8L'}{\pi} \times \frac{P_f(d+2s)}{(d+2s)^4 - d^4} \quad (1)$$

where R_f is the three point bending strength (MPa), P_f is the fracture stress (N), L' is the distance between supporting jigs (mm), d is the inner diameter of tubular support at fracture point (mm), and s is the wall thickness of the support at fracture point (mm). The several strength data obtained from Eq. (1) can be compared regardless of the shape (dimensions) of the tubular supports.

The corrosion resistance of the support was characterized by analyzing the strength of supports after immersing in 1 wt.% NaOH solution (pH value more than 14) and 1 wt.% HNO_3 solu-

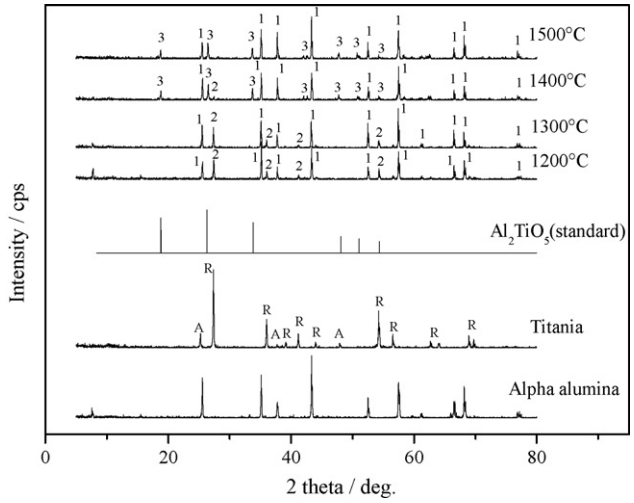

Fig. 3. XRD patterns of starting powders and support A85/15(AQ) sintered at different temperatures (A, anatase; R, rutile; 1, alpha-alumina; 2, rutile; 3, aluminum titanate).

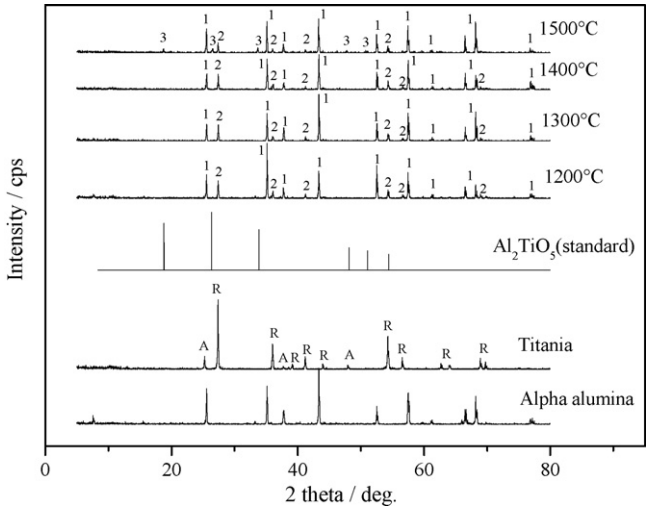

Fig. 4. XRD patterns of starting powders and support A85/15 sintered at different temperatures (A, anatase; R, rutile; 1, alpha-alumina; 2, rutile; 3, aluminum titanate).

tion (pH value less than 1) for a certain period of time. Sealed PTFE beakers containing the NaOH and HNO_3 solution, respectively were placed into a thermostatic water bath at a constant temperature of 90 °C.

3. Results and discussion

3.1. Microstructure evolution of the Al_2O_3/TiO_2 composite supports as function of sintering temperature

Fig. 2 shows SEM photos of the quenched support A85/15(AQ) sintered at various temperatures. Corresponding to each SEM photo, Al and Ti micromaps reflect the distribution of Al_2O_3 and TiO_2 in the support. It can be seen in Fig. 2a that coarse-grained Al_2O_3 and fine aggregated TiO_2 grains are present after sintering at 1300 °C. As the sintering temperature increased, the amount of fine TiO_2 particles decreased (Fig. 2b). In the corresponding Al and Ti micromaps (Fig. 2b-Al and -Ti), a substance containing both elements Al and Ti ("S" in Fig. 2) is visible. When the sintering temperature reached 1500 °C, the SEM photo in Fig. 2c shows that the particles impinged onto each other and TiO_2 is hardly distinguishable besides alumina. Meanwhile a considerable quantity of the substance containing both elements Al and Ti is present in the corresponding micromaps ("S" in Fig. 2c-Al and -Ti). The XRD patterns (Fig. 3) of support A85/15(AQ) indicated that the substance "S" on the micromaps can be ascribed to aluminum titanate (Al_2TiO_5).

The phase composition of starting powders, together with the support A85/15(AQ) sintered at various temperatures is depicted in Fig. 3. With increasing sintering temperature the phase composition of the support transformed in the following sequence: $Al_2O_3 + TiO_2$ (1200 °C and 1300 °C) → $Al_2O_3 + TiO_2 + Al_2TiO_5$ (1400 °C) → $Al_2O_3 + Al_2TiO_5$ (1500 °C). Fig. 4 shows XRD patterns of sintered and furnace-cooled supports A85/15. If compared with the corresponding XRD patterns of support A85/15(AQ) in Fig. 3, the Al_2O_3/TiO_2 composite support cooled down in the furnace at a rate of 3 °C/min always consists of TiO_2 and Al_2O_3 irrespective of the sintering temperature except a small amount of Al_2TiO_5 present in the support sintered at 1500 °C.

It was reported[18,23] that two concurrent processes occur during sintering of an Al_2O_3/TiO_2 mixture, i.e. densification and a solid-state reaction between Al_2O_3 and TiO_2. At temperatures above 1280 °C, Al_2O_3 reacts with TiO_2 under the formation of Al_2TiO_5, which is also confirmed by the Al_2O_3–TiO_2 phase diagram.[24] During cooling to ambient temperature the aluminum titanate decomposes into Al_2O_3 and TiO_2.[15] It should be noted that the formation temperature of Al_2TiO_5 in this paper was observed only around 1400 °C, which is higher than the reported value of 1280–1300 °C.[15,18,23] This is probably because the particle size of Al_2O_3 ($D_{50} = 30$ μm) and TiO_2 ($D_{50} = 0.5$ μm) used in this paper was different from the Al_2O_3–TiO_2 powder mixtures (Al_2O_3 ($D_{50} < 0.4$ μm)–TiO_2 ($D_{50} = 1.5$ μm)[23] and Al_2O_3

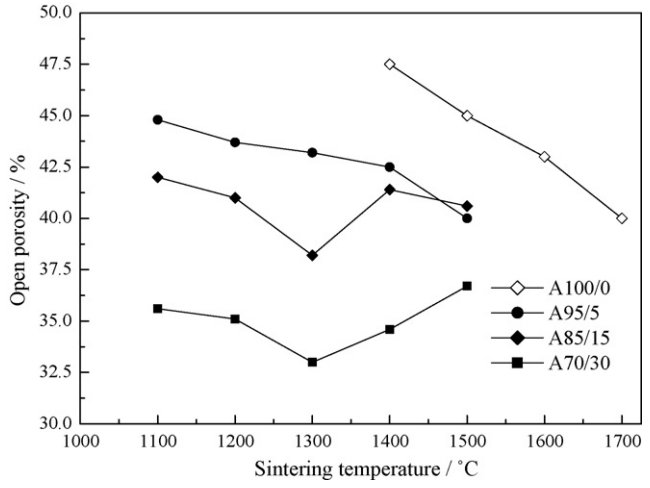

Fig. 5. The variation of porosity of supports as function of sintering temperature (dwell time: 2 h).

Table 2
Average pore size (μm) of supports with different Al_2O_3/TiO_2 composition sintered at various temperatures.

Sintering temperature (°C)	A95/5	A85/15	A70/30
1100	–	–	0.9
1200	4.7	3.1	1.4
1300	6.4	4.4	2.3
1400	6.5	6.8	4.6
1500	6.1	6.3	6.3

"–" indicates the strength of support is too low to be characterized.

($D < 0.4$ μm)–TiO_2 ($D_{50} = 13$ μm)[18]) studied by Freudenberg and Mocellin. In addition, the higher formation temperature of Al_2TiO_5 reported here can also be ascribed to the low extrusion pressure (4 MPa) compared with a pressure of 250 MPa in the sample fabrication by using an isostatic pressing shaping method.[18,23] However it can also be the case that the formation of Al_2TiO_5 in support A85/15(AQ) starts at lower temperature (i.e. 1300 °C), but that the amount was very low and it decomposes again into Al_2O_3 and TiO_2 during quenching.

Freudenberg and Mocellin[23] proposed that the formation of Al_2TiO_5 in an Al_2O_3/TiO_2 mixture was the result of Al transport through the TiO_2 layer and reacted with TiO_2. That is, TiO_2 has a double role as a reactant and as rapid Al-transporting medium, which leads to the Al_2TiO_5 formation. The formation of Al_2TiO_5 is very helpful in accelerating the sintering rate of the Al_2O_3/TiO_2 composite support, so sinter necks between alumina particles with size of ~30 μm could be formed at a relatively low temperature.

3.2. Effect of sintering temperature on support properties

The open porosity of the supports A100/0–A70/30 sintered at various temperatures and furnace-cooled is displayed in Fig. 5. Because of the extremely low mechanical strength of the support A100/0 sintered below 1400 °C, only the porosity of this support sintered above 1400 °C is displayed. It is obvious that doping titania into alumina support results in a better sintering behaviour as evidenced by the decrease in support porosity with increasing titania content. In the case of support A95/5, it can be seen that the open porosity decreased with increasing sintering temperature. However, an irregular result for the variation of the open porosity is apparent for supports A85/15 and A70/30.

As was mentioned in Section 3.1, the heat treatment of an Al_2O_3/TiO_2 composite support consists of two concurrent processes of densification and reaction. The theoretical density of β-Al_2TiO_5, α-Al_2O_3 and rutile is 3.70 g/cm^3, 3.90 g/cm^3 and 4.25 g/cm^3, respectively. Therefore, the reaction between Al_2O_3 and TiO_2 is accompanied by an 11% molar volume increase.[23] The open porosity of the support (A95/5–A70/30) decreased regardless of the composition of Al_2O_3/TiO_2 because only densification took place in the supports below 1300 °C.

Table 3
Three point bending strength (MPa) of supports with different Al_2O_3/TiO_2 composition sintered at various temperatures.

Sintering temperature (°C)	A95/5	A85/15	A70/30
1100	–	7.3	23.1
1200	–	18.1	40.7
1300	13.1	34.1	49.4
1400	18.2	32.7	13.2
1500	26.3	26.2	1.6

"–" indicates the strength of support is too low to be determined.

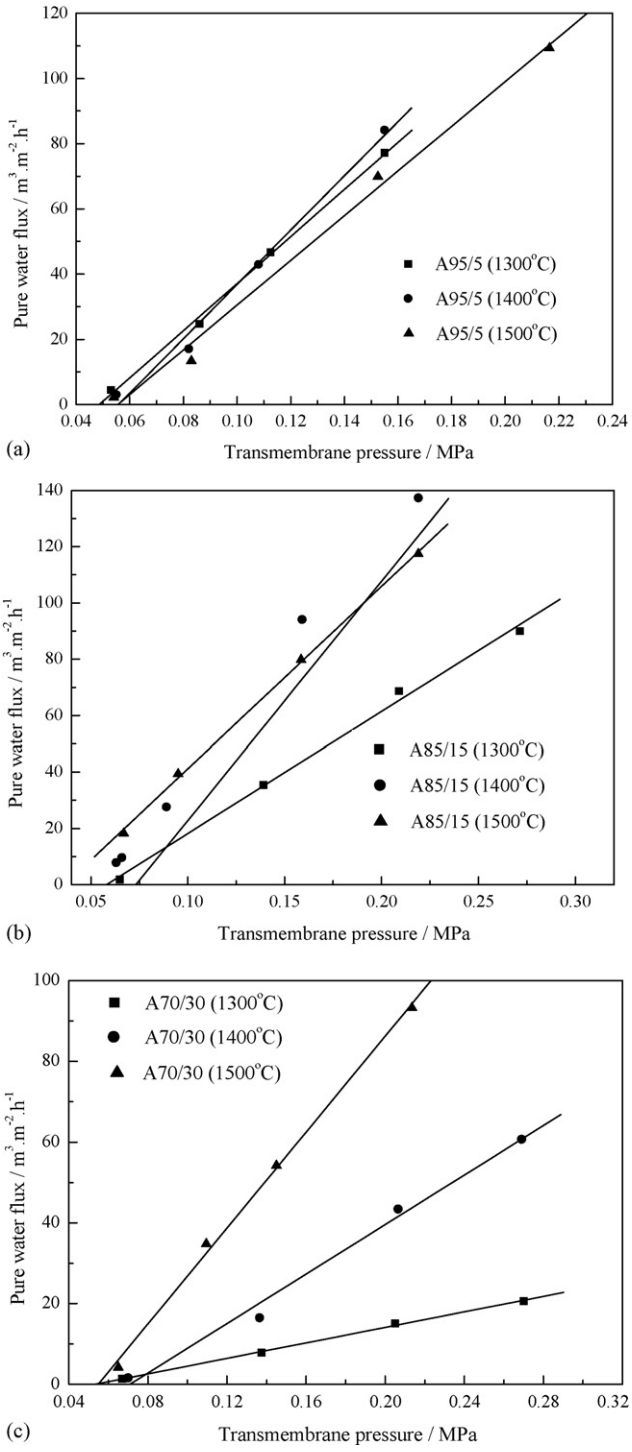

Fig. 6. Pure water flux of supports sintered at various temperatures versus transmembrane pressure: (a) A95/5, (b) A85/15, and (c) A70/30 (dwell time: 2 h).

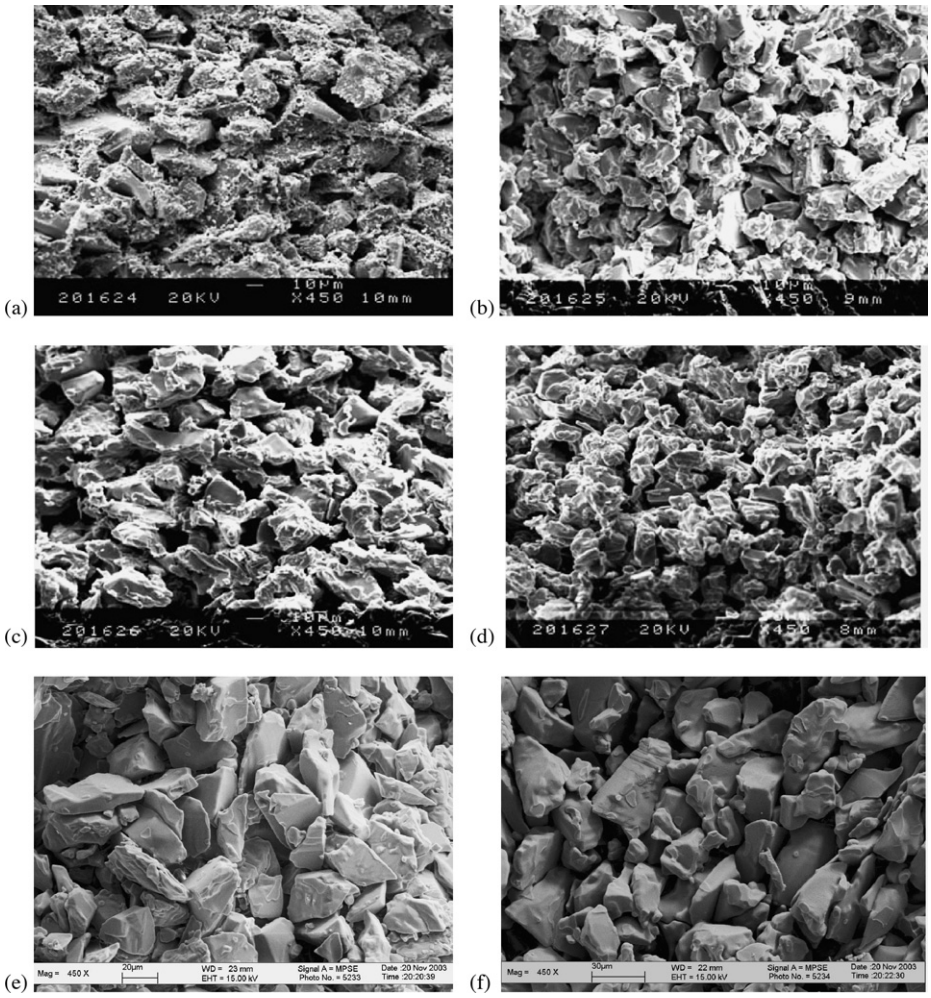

Fig. 7. SEM sectional photos of the support A85/15 sintered at various temperatures of (a) 1200 °C, (b) 1300 °C, (c) 1400 °C, (d) 1500 °C, as compared with the support A100/0 sintered at (e) 1600 °C and (f) 1700 °C, respectively.

When the sintering temperature is higher than 1300 °C, the porosity of Al_2O_3/TiO_2 composite support will decrease further because of the densification process. However, the simultaneously occurring volume expansion caused by the Al_2O_3/TiO_2 reaction hampers this densification. Therefore, the amount of Al_2TiO_5 formed in the support plays a key role in the variation of the open porosity. If the porosity reduction caused by densification does not match with the volume expansion due to aluminum titanate formation, the open porosity of the support would decrease (in the case of support A95/5) or increase (in the case of support A70/30) as the sintering temperature increased. If porosity reduction matches the volume expansion due to the formation of the aluminum titanate, the porosity of the support does not vary obviously with increasing sintering temperature (in the case of support A85/15 sintered at 1400 °C and 1500 °C).

In Table 2 average pore sizes of supports A95/5–A70/30 sintered at various temperatures are given. Except for the support A95/5 and A85/15 sintered at 1500 °C, it can be seen that the pore size of support increases as the sintering temperature increases irrespective of the TiO_2 doping amount. Fine-grained TiO_2 occupying the space formed by the packing of coarse-grained Al_2O_3 should be responsible for the smaller pore size of support sintered at low temperatures (1200 °C or lower). As the sintering temperature increases, the disappearance of TiO_2 and formation of Al_2TiO_5 accordingly increase the distance between Al_2O_3 particles and result in an increase in pore size.[25] It should be noted that the pore size of the supports A95/5 and A85/15 sintered at 1500 °C is (slightly) smaller than that of those supports sintered at 1400 °C. This result can be attributed to the densification of a support consisting of Al_2O_3 and Al_2TiO_5 after the completion of reaction of Al_2O_3–TiO_2 composite at 1400 °C.

Fig. 6 gives the pure water flux of the support as function of transmembrane pressure. By comparison with Fig. 5 and Table 2, it is obvious that the pore size has a stronger impact on pure water flux of support than porosity.

Table 3 shows three point bending strengths of supports sintered at different temperatures. The strength of support A95/5 increased with sintering temperature. Compared with support A95/5, the mechanical strength of support A85/15 sintered below 1400 °C exhibits the same tendency. It is worthwhile to note that a higher temperature of 1500 °C leads to a lower mechanical strength for the support A85/15. With respect to the support A70/30, a maximum in strength of 49.4 MPa is obtained at a sintering temperature of 1300 °C. The higher

sintering temperature above 1300 °C impairs the strength of support A70/30 greatly. The same phenomenon observed in the literature[18,19] indicates that the sintering temperature of Al_2O_3/TiO_2 system must not be higher than 1275 °C because the appearance of Al_2TiO_5 would impair the mechanical strength of the Al_2O_3/TiO_2 composite. Our results confirm the previous observations[23] and find that the amount of Al_2TiO_5 plays an important role in determining the mechanical strength of Al_2O_3/TiO_2 composite supports. The more the Al_2TiO_5 formed in the Al_2O_3/TiO_2 composite, the lower the strength of the supports. Therefore, to obtain a macroporous membrane supports exhibit both high mechanical strength and high permeability, the sintering temperature for support A85/15 should not be higher than 1400 °C.

Fig. 7 shows the microstructure evolution for support A85/15 at different sintering temperatures, together with SEM images for support A100/0 obtained after sintering at 1600 °C and 1700 °C. Support A85/15 shows that the fine particles (TiO_2) and coarse-grained Al_2O_3 are aggregated at a sintering temperature of 1200 °C. The fine TiO_2 particles gradually disappeared and most of the particles impinged onto each other as the sintering temperature elevated. With respect to the support sintered above 1400 °C, TiO_2 particles can hardly be discriminated and sinter necks between alumina particles are visible. However, as far as the pure alumina support is concerned, there is only a slight difference between the microstructure of supports sintered at 1600 °C and 1700 °C (Fig. 7e and f). Only a packing of alumina particles is visible and no obvious sinter necks could be observed even if it is sintered at 1700 °C, as evidenced by the low mechanical strength of this support (<10 MPa). With respect to support A85/15, it is worthwhile to note that the sinter neck area increased when sintering at 1500 °C. However, the lower strength of this support than that of 1400 °C sintered one confirmed the negative influence of the formation of Al_2TiO_5 on the mechanical strength of the Al_2O_3/TiO_2 composite supports.

Chemical stability tests for A85/15 (sintered at 1400 °C for 2 h) were performed by immersing the support into 1 wt.% NaOH solution (90 °C) and 1 wt.% HNO_3 solution (90 °C), respectively for a certain period of time. The results shown in Fig. 8a and b indicate that the support exhibits an excellent chemical stability towards NaOH and HNO_3 solutions (90 °C) even after a corrosion test for 720 h.

According to the above investigations, the macroporous composite support A85/15 sintered at 1400 °C for 2 h with integrated properties of permeability, mechanical and chemical stability was chosen for microfiltration (MF) membranes preparation. A well-dispersed and stable submicron alumina suspension was synthesized and subsequently coated onto the support A85/15 via a dip-coating method and calcined at 1300 °C afterwards. The mean pore size of the MF membrane coated on the composite support A85/15 was 0.7 μm and more than 90% pores were in the range of 0.4–2 μm, as evidenced by Fig. 9. The pure water flux of the MF layer was 10 $m^3\ m^{-2}\ h^{-1}\ bar^{-1}$. Microstructures of the surface and the fracture section of the membrane shown in Fig. 10a and b confirmed a crack-free membrane layer with a thickness in the range of 30–40 μm.

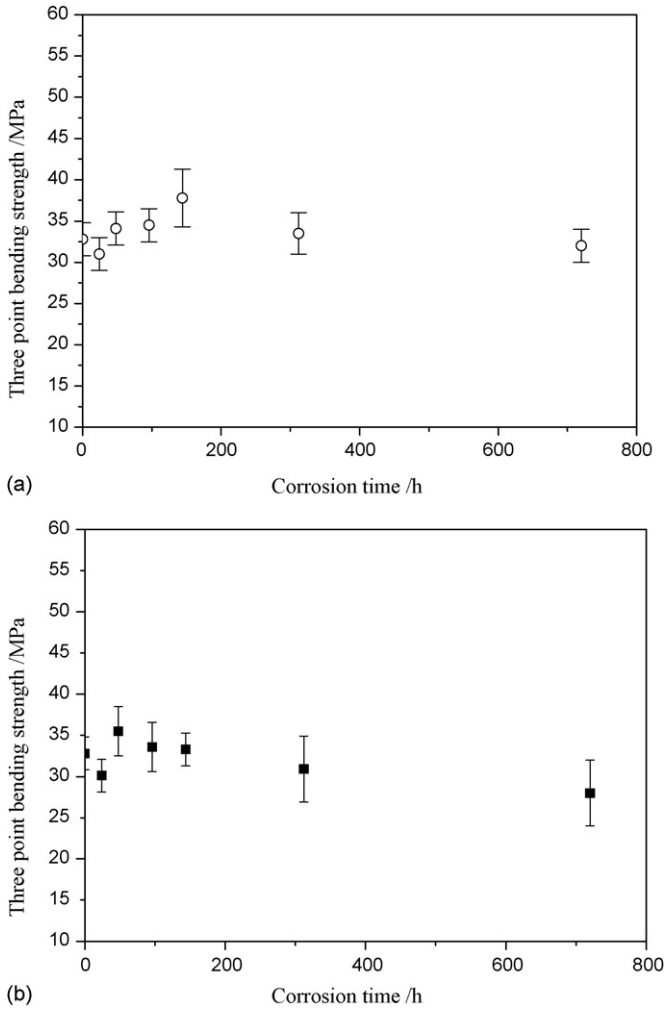

Fig. 8. Variation of three point bending strength of support A85/15 as function of time immersed in corrosive liquids (at 90 °C): (a) 1 wt.% NaOH solution and (b) 1 wt.% HNO_3 solution.

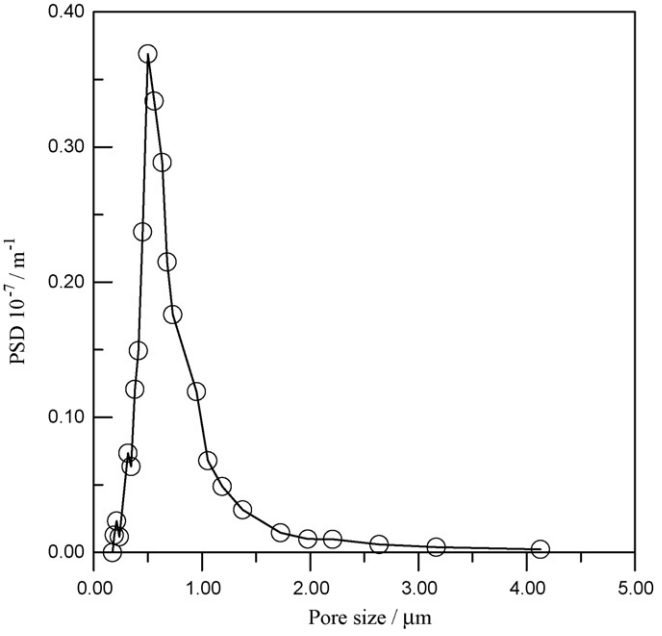

Fig. 9. Pore size distribution of the MF membrane coated on supports A85/15.

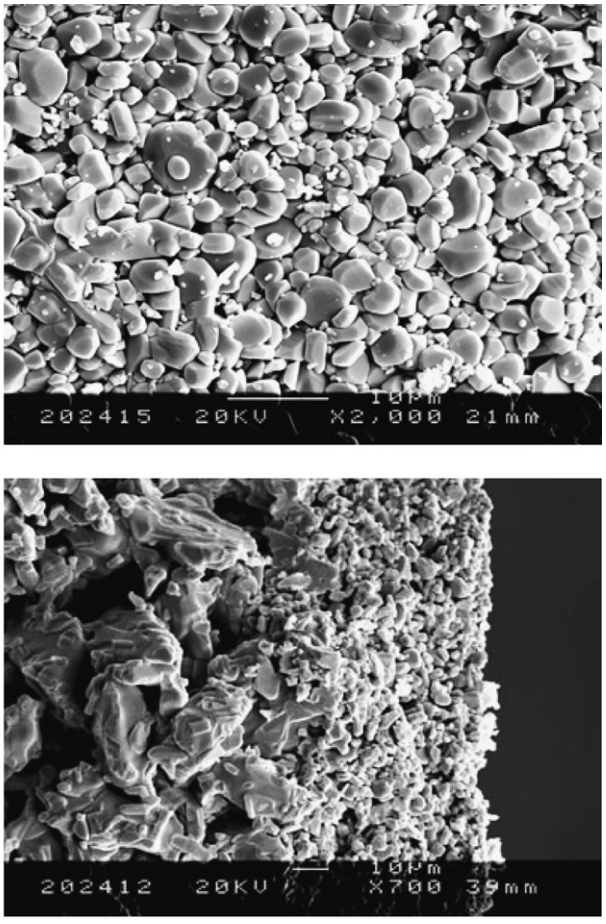

Fig. 10. SEM photos of surface (a) and fractured (b) section of the MF membrane.

4. Conclusions

(1) A tubular macroporous ceramic support consisting of alumina and titania showing sufficient permeability and high mechanical strength was prepared by extrusion and subsequent sintering at 1400 °C for 2 h. This low sintering temperature can largely reduce the cost of the macroporous membrane support.

(2) The formation mechanism of the support was studied in detail by SEM, EDX micromapping and XRD, which confirmed that two concurrent processes occurred during the sintering process of these Al_2O_3/TiO_2 composite support, i.e. densification and solid-state reaction, The formation of Al_2TiO_5 depends on sintering temperature and has a strong impact on the properties of the Al_2O_3/TiO_2 composite support, especially with regard to the mechanical strength.

(3) The effect of the sintering temperature on the properties of Al_2O_3/TiO_2 composite support was investigated. The results show that the support with a composition of 85 wt.% Al_2O_3/15 wt.% TiO_2 sintered at 1400 °C for 2 h exhibits both high permeability (with a pure water flux of 45 $m^3\,m^{-2}\,h^{-1}\,bar^{-1}$) and sufficient mechanical strength (32.7 MPa), together with excellent corrosive resistance towards hot NaOH and HNO_3 solutions (1 wt.%, 90 °C).

(4) A crack-free MF membrane with a pore size of ~0.7 μm was successfully prepared via dip-coating method by using the above-mentioned Al_2O_3/TiO_2 composite support.

Acknowledgements

The author would like to thank the financial support of the National Basic Research Program (973 Program, Code: 2009CB623400) and the National Natural Science Foundation of China (20906047). This work was also sponsored by State Key Laboratory of Chemical Engineering (No. SKL-ChE-09A01) and the Scientific Research Foundation for the Returned Overseas Chinese Scholars.

References

1. Mallada R, Menéndez M. *Inorganic membranes synthesis, characterization and applications*. Amsterdam, The Netherlands: Elsevier Press; 2008 p. 177–215.
2. Burggraaf AJ, Cot L. *Fundamentals of inorganic membrane science and technology*. Amsterdam, The Netherlands: Elsevier Science BV; 1996 p. 619–634.
3. Hsieh HP. *Inorganic membranes for separation and reaction*. Amsterdam, The Netherlands: Elsevier Science BV; 1996 p. 569–581.
4. Biesheuvel PM, Verweij H. Design of ceramic membrane supports: permeability, tensile strength and stress. *J Membr Sci* 1999;**156**:141–52.
5. Maebashi N, Kanagawa. Ceramic filter and process for making it. US Patent 5,098,571; 1992.
6. Dong YC, Feng XY, Dong DH, Wang SL, Yang JK, Gao HF, et al. Elaboration and chemical corrosion resistance of tubular macro-porous cordierite ceramic membrane supports. *J Membr Sci* 2007;**304**(1–2):65–75.
7. Chen GL, Qi H, Xing WH, Xu NP. Direct preparation of macroporous mullite supports for membranes by in situ reaction sintering. *J Membr Sci* 2008;**318**(1–2):38–44.
8. Wang HT, Liu XQ, Chen FL. Kinetics and mechanism of a sintering process for macroporous alumina ceramics by extrusion. *J Am Ceram Soc* 1998;**81**(3):781–4.
9. Khemakhem S, Larbot A, Amar Ben, New R. Ceramic microfiltration membranes from Tunisian natural materials: application for the cuttlefish effluents treatment. *Ceram Int* 2009;**35**(1):55–61.
10. Shimai S, Imura X, Okamoto K, Muto T. Ceramic filter and manufacturing method therefor. US Patent 5,405,529; 1995.
11. Franklin SA, Rand B. Partial sintering in porous alumina refractories: effect of size distribution on microstructure and elastic modulus. *Br Ceram Trans* 1996;**95**(3):93–8.
12. Wang YH, Cheng JG, Liu XQ, Meng GY, Ding YW. Preparation and sintering of macroporous ceramic membrane support from titania sol-coated alumina powder. *J Am Ceram Soc* 2008;**91**(3):825–30.
13. Wang YH, Zhang Y, Liu XQ, Meng GY. Sol-coated preparation and characterization of macroporous alpha-Al_2O_3 membrane support. *J Sol-Gel Sci Technol* 2007;**41**(3):267–75.
14. Asaeda M, Sakou Y, Yang JH, Shimasaki K. Stability and performance of porous silica–zirconia composite membranes for pervaporation of aqueous organic solutions. *J Membr Sci* 2002;(209):163–75.
15. Kato E, Daimon K, Takahashi J. Decomposition temperature of β-Al_2TiO_5. *J Am Ceram Soc* 1980;**63**(5–6):355–6.
16. Prodanovic D, Zivanovic B. Effect of TiO_2 on phase formation in the Al–Si–Al_2O_3 system. *Interceram* 1996;**45**(1):21–6.
17. Kingery WD, Bowen HK, Uhlmann DR. *Introduction to ceramics*. 2nd ed. John Wiley & Sons, Inc; 1976.
18. Freudenberg B, Mocellin A. Aluminum titanate formation by solid-state reaction of coarse Al_2O_3 and TiO_2 powders. *J Am Ceram Soc* 1988;**71**(1):22–8.
19. Castillon R, Lavandare JP. Monolithic ceramic supports for filtering membranes. US Patent 5,415,775; 1995.

20. Wang YH, Zhang Y, Liu XQ, Meng GY. Microstructure control of ceramic membrane support from corundum–rutile powder mixture. *Powder Technol* 2006;**168**(3):125–33.
21. Huang P, Xing WH, Xu NP, Shi J. Pore size distribution determination of inorganic microfiltration membrane by gas bubble press method. *Technol Water Treat* 1996;**22**:80 [in Chinese].
22. Collection of Chinese National Standards (22). *Asbestos–cement pressure pipe for water transmission*. Beijing: Chinese Standards Press; 1986. p. 657–665 [in Chinese].
23. Freudenberg B, Mocellin A. Aluminum titanate formation by solid-state reaction of fine Al_2O_3 and TiO_2 powders. *J Am Ceram Soc* 1987;**70**(1):33–8.
24. Levin EM, Mc Murdie HF. *Phase diagrams for ceramists*. Columbus, OH: The American Ceramic Society; 1975. Fig. 4376 Supplement.
25. Leblud C, Anseau MR, Di Rupo E, Cambier F, Fierens P. Reaction sintering of ZnO–Al_2O_3 mixtures. *J Mater Sci Lett* 1981;**16**(2):539–44.